

Chaos thresholds in finite Fermi systems

P. G. Silvestrov

Budker Institute of Nuclear Physics, 630090 Novosibirsk, Russia

(Received 26 May 1998)

The development of quantum chaos in finite interacting Fermi systems is considered. At sufficiently high excitation energy the direct two-particle interaction may mix into an eigenstate the exponentially large number of simple Slater determinant states. Nevertheless, the transition from Poisson to Wigner-Dyson statistics of energy levels is governed by the effective high-order interaction between states very distant in the Fock space. The concrete form of the transition depends on the way one chooses to work out the problem of factorial divergence of the number of Feynman diagrams. In the proposed scheme the change of statistics has a form of narrow phase transition and may happen even below the direct interaction threshold.

[S1063-651X(98)13610-3]

PACS number(s): 05.45.+b, 73.23.-b, 71.70.-d

I. INTRODUCTION

The investigation of chaotic properties of finite interacting quantum systems has now a few decades history [1–7]. The random matrix theory, originally introduced for modeling this problem, adequately describes the statistics of complicated high-energy excitations (see Ref. [8] for an extensive review). However, the concrete mechanism of developing the chaotic behavior in the finite Fermi system with increasing excitation energy still requires further understanding. The interest in this problem has even increased in recent years in particular due to the recent explosion of activity in the field of mesoscopic physics (quantum dots, atomic clusters, helium droplets, etc.). The experimental observation of electronic excitations in quantum dots [9] has stimulated progress [10–14] in the theoretical investigation of chaotic disintegration of single-electron excitations in this systems. The single-particle excitations, being most easily produced experimentally, constitute an important part of the Hilbert space of the complicated system. However, the number of such states is exponentially small compared to the total number of excited states. The onset of chaos in the majority of many-particle states is the subject of this paper.

We will consider finite but sufficiently large Fermi systems. The particles are supposed to occupy almost all orbitals below the Fermi energy ϵ_F of the mean field single-particle Hamiltonian [15]. The averaged single-particle level spacing is $\Delta \ll \epsilon_F$. We will denote as simple states the single Slater determinant states having definite occupation numbers (0 or 1) of all orbitals. The simple states are mixed by the two-particle interaction and the matrix elements V are supposed to be small and Gaussian random

$$\overline{V^2} = \Delta^2/g^2, \quad g \gg 1. \tag{1}$$

Here g may be interpreted as dimensionless conductance in the case of a quantum dot [11,12]. This simple model was in fact introduced long ago in Refs. [2,3].

Due to the weak interaction (1), the low-energy excited states are almost unperturbed. With the increase of energy \mathcal{E} the density of states grows rapidly and the exact wave functions at $\mathcal{E} \gg \Delta$ are formed by many chaotically mixed simple

states. However, this chaotization of excited states proceeds in a very nonuniform and complicated way. For illustration we have shown in Fig. 1 different energy scales relevant to this problem.

The complexity of the excited state is usually characterized by the inverse participation ratio (IPR) $I = \sum_k |\psi_i(k)|^4$, where $\psi_i(k)$ is the amplitude of the k th simple excitation in the i th exact wave function. Physically I is the effective inverse number of simple states mixed into the exact one.

While the density of single-particle states $\nu_1 = 1/\Delta$ does not depend on energy, the total density grows extremely fast with \mathcal{E} being $\nu_{total} \sim \Delta^{-1} \exp(2\pi\sqrt{\mathcal{E}/6\Delta})$ [16]. We use large \mathcal{E} for the total energy of the many-particle configuration and small ϵ for the energy of single-particle orbitals. Due to the huge number of states (the analog of the microcanonical ensemble in thermodynamics) the averaged occupation number for a given orbital for an arbitrarily chosen “typical” simple state is given by the usual Fermi-Dirac distribution

$$f(\epsilon - \epsilon_F) = \overline{n(\epsilon)} = \left(\exp \left[\frac{\epsilon - \epsilon_F}{T} \right] + 1 \right)^{-1}, \tag{2}$$

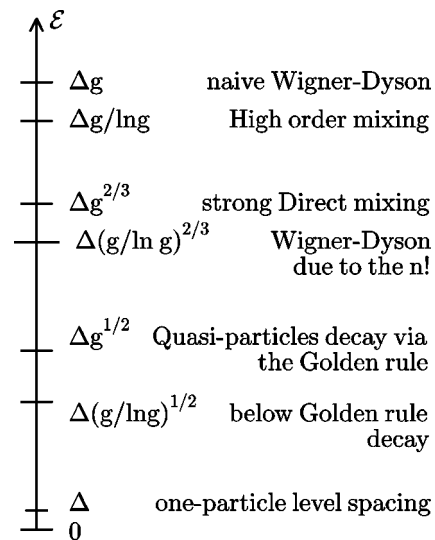


FIG. 1. Different energy scales corresponding to chaotization of single- or many-particle excited states.

where $T = \sqrt{6\mathcal{E}\Delta}/\pi$ [17]. Note that we still have not taken into account the interaction V , but only explore the wide statistics of single-Slater-determinant states.

The low-energy thresholds in Fig. 1 correspond to the decay of single quasiparticles. Quasiparticles in a quantum dot may be seen as peaks broadened by the interaction (bunches of δ peaks) in the one-particle spectral density up to the energy $\varepsilon \sim \Delta g$ [10]. Above $\varepsilon \sim \Delta\sqrt{g}$ the broadening arises due to a decay of the quasiparticle into two particles and one hole and may be explained by the Fermi golden rule. Below this energy the width predicted by golden rule turns out to be smaller than three-particle level spacing. However, as it was shown recently [12] up to energy $\varepsilon \sim \Delta\sqrt{g/\ln g}$, the quasiparticle disintegration still proceeds through the effective interaction with the many excited particle and hole states. A nonuniform distribution of the matrix elements of the effective interaction in this case leads to a very unusual distribution of spacings between the peaks and widths of the bunches [14].

The original intention of this research was to apply the methods developed for the description of quasiparticle disintegration for the investigation of the full spectrum of a complicated system. However, the onset of chaos in the many-particle excitations provided us with a number of surprising effects not present in the single-quasiparticle case. Only the estimate of the effective high-order matrix element in Sec. III may be considered as a straightforward generalization of the analogous estimate in Ref. [14]. In Sec. II we will show how the direct interaction between particles may mix into one wave function an exponentially large number of simple states even inside the region of the Poissonian spectrum. In Sec. III we consider the self-consistent scheme of the onset of chaos based on the analysis of the scaling behavior of the direct and effective interaction. However, in Sec. IV we propose another scenario of the Wigner-Dyson transition caused by the factorial divergence of the high-order interaction. The detailed comparison of the features of these two scenarios is given in Sec. V.

II. MIXING BY THE DIRECT INTERACTION

For a weak interaction the strong mixing of different quantum states may take place only if their energies occasionally turn out to be very close. Therefore, consider first only two states $|i\rangle$ and $|f\rangle$ with an energy difference ε connected by the matrix element V . The simple calculation [18] gives the IPR for the exact wave function $\alpha|i\rangle + \beta|f\rangle$,

$$I = \alpha^4 + \beta^4 = 1 - \frac{2V^2}{\varepsilon^2 + 4V^2}. \quad (3)$$

Let us fix the state $|i\rangle$ and consider a set of states $|f\rangle$ with a density $dn/d\varepsilon = \Delta_f^{-1}$. It is convenient to introduce the intermediate scale ε_0 : $|V| \ll \varepsilon_0 \ll \Delta_f$. With the probability $1 - 2\varepsilon_0/\Delta_f$ there are no final states falling into the strip $-\varepsilon_0 < \varepsilon < \varepsilon_0$ and $I = 1$ up to a negligible correction $\sim V^2/\Delta_f\varepsilon_0$. With the small probability $2\varepsilon_0/\Delta_f$ one of the states $|f\rangle$ enters the strip. In order to find I in this case one has to average Eq. (3) over the interval of energy

$$\int_{-\varepsilon_0}^{\varepsilon_0} \left(1 - \frac{2V^2}{\varepsilon^2 + 4V^2} \right) \frac{d\varepsilon}{2\varepsilon_0} = 1 - \frac{2\pi|V|}{2\varepsilon_0} \quad (4)$$

and then average the $|V|$ over the ensemble of matrix elements. Combining the two contributions one finds

$$I = 1 - \frac{2\varepsilon_0}{\Delta_f} + \frac{2\varepsilon_0}{\Delta_f} \left(1 - \frac{2\pi|V|}{2\varepsilon_0} \right) = 1 - 2\pi \frac{|V|}{\Delta_f}. \quad (5)$$

This simple formula is basic for our perturbative estimates. The averaging of the modulus of V for strongly non-Gaussian high-order effective matrix elements will be the main subject of Sec. III.

The goal of this paper is to consider the mixing of complicated excited states. Occupation numbers for these states are described by Eq. (2). The density of directly accessible states or the density of pairs of occupied 1,2 and unoccupied 3,4 states with $\varepsilon_1 + \varepsilon_2 = \varepsilon_3 + \varepsilon_4$, which may be connected directly by the interaction, is

$$\frac{1}{\Delta_2} = \frac{1}{(2!)^2} \int \delta\left(\sum x_i\right) \prod_{i=1}^4 f_i \frac{dx_i}{\Delta} = \frac{T^3}{\Delta^4} \frac{\pi^2}{6}. \quad (6)$$

Here $f_i = f(x_i)$ (2), $x_{1,2} = \varepsilon_{1,2} - \varepsilon_F$, $x_{3,4} = \varepsilon_F - \varepsilon_{3,4}$, and we have used that $1 - f(x) = f(-x)$. The factor $(2!)^{-2}$ accounts for the identical initial and final particles. It is easy now to use Eq. (5) to find the IPR. However, this result may be even further improved. Equation (5) with $\Delta_f = \Delta_2$ describes the situation when only for one 2×2 transition $1,2 \rightarrow 3,4$ the energy difference turns out to be of the same order of magnitude as the matrix element. In the second order in V the leading contribution to I is given by a double event $1,2 \rightarrow 3,4$ and $5,6 \rightarrow 7,8$. However, as long as none of the orbitals $5-8$ coincides with any of $1-4$ these two corrections are completely independent and corresponding contributions to I should be simply multiplied. Effectively, all one-particle states are chosen from $\sim T/\Delta$ orbitals around ε_F . Therefore, if the number of couples of pairs falling into the energy interval $\sim |V|$ is small compared to $\sim T/\Delta$ one may neglect the interference between different direct transitions. Again, we may introduce the intermediate scale ε_0 : $|V| \ll \varepsilon_0$. The number of directly accessible final states is $2\varepsilon_0/\Delta_2 \gg 1$, but until $\varepsilon_0/\Delta_2 \ll T/\Delta$ the IPR is found simply as a product over these channels

$$\begin{aligned} I &= \left(1 - 2\pi \frac{|V|}{2\varepsilon_0} \right)^{2\varepsilon_0/\Delta_2} = \exp\left\{ -2\pi \frac{|V|}{\Delta_2} \right\} \\ &= \exp\left\{ -\frac{4\sqrt{3}}{\sqrt{\pi g}} \left(\frac{\mathcal{E}}{\Delta} \right)^{3/2} \right\}. \end{aligned} \quad (7)$$

Here we have averaged $|V|$ for the Gaussian random interaction (1). This result is valid for $\Delta/g \ll \Delta_2 T/\Delta$ or $T \ll \Delta\sqrt{g}$. The exponentiation of the IPR is a direct consequence of the two-particle character of the interaction. It would be very inconvenient to investigate such effects if one considers the Hamiltonian of the system as a random (sparsed) matrix in the full Hilbert space. Surprisingly, to the

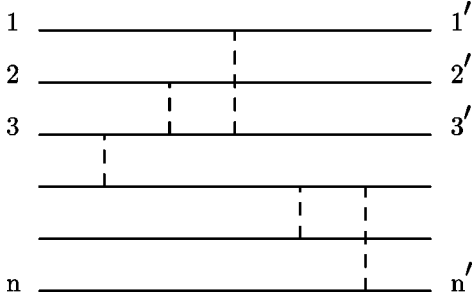


FIG. 2. Tree-type diagram contributing to the high-order effective matrix element. The screened Coulomb interaction is shown by dashed lines.

best of my knowledge, the simple effect (7) has not been considered yet, e.g., for the description of the excitations in complex nuclei.

Due to Eq. (7), at $\mathcal{E} > \Delta g^{2/3}$ the number of components in a typical wave function becomes exponentially large. However, within the range of validity of Eq. (7) only a small (also exponentially) part of close energy levels is mixed in any exact eigenstate. Therefore, this simple effect is not enough for the creation of full quantum chaos.

III. HIGH-ORDER EFFECTIVE INTERACTION

Corrections to Eq. (7) arise after taking into account the high-order effective interaction between three-particle states, and then four-particle states, etc. The example of the corresponding tree-type Feynman diagram is shown in Fig. 2. The tree-type diagrams are maximally enhanced due to a wide statistics of initial and final orbitals. Contributions from the diagrams with closed loops are small, such as some power of Δ/T . The generalization of Eq. (6) for the case of the n -particle interaction gives

$$\frac{1}{\Delta_n} = \int \frac{\delta\left(\sum x_i\right)}{(n!)^2} \prod_{i \leq 2n} f_i \frac{dx_i}{\Delta} = \frac{(2\pi T)^{2n-1}}{\pi n(2n)! \Delta^{2n}}. \quad (8)$$

Again $(n!)^{-2}$ accounts for the identical fermions. Note that $(2n)! \sim 2^{2n}(n!)^2$ and therefore the integration over the energies x_i does not lead here to any $n!$ suppression. This is in strict contrast with what happens for the decay of quasiparticles [14], where the main suppression of the density of final states ν_n arose due to the integration over the energies of final particles.

The calculation of the averaged modulus of the effective matrix element entering both Eqs. (5) and (7) turns out to be sufficiently more complicated. The simplest variant of the effective interaction is given by the three-particle interaction arising in the second order of perturbation theory

$$V_{eff}^{(3)} = \sum_2 \frac{V_{12}V_{23}}{\varepsilon_1 - \varepsilon_2}. \quad (9)$$

Formally this interaction mixes together three states $|1\rangle$, $|2\rangle$, and $|3\rangle$. The use of the concept of an effective interaction requires that the admixture of the intermediate state $|2\rangle$ in the total wave function is small compared to those of $|1\rangle$ and $|3\rangle$. This means that $V_{12}, V_{23} \ll |\varepsilon_1 - \varepsilon_2| \approx |\varepsilon_2 - \varepsilon_3|$. The

contribution to the averaged IPR from strongly mixed (almost degenerate) $|1\rangle$, $|2\rangle$, and $|3\rangle$ should be considered separately, but this correction is small, e.g., $1/\ln g$, compared to the total contribution of the effective interaction. On the other hand, we will be interested in the tail of the distribution of the effective matrix elements. For Gaussian distributed V [Eq. (1)] the probability to find a large individual matrix element of the original two-particle interaction is exponentially small. The large matrix elements appear if one term in the sum in Eq. (9) occasionally has an anomalously small denominator $|\varepsilon_1 - \varepsilon_2| \ll \Delta$. All the other (random) contributions in the sum in this case may be neglected for $\ln g \gg 1$. The result of this lengthy discussion may be summarized in the formula for the probability distribution for the effective matrix element (9)

$$P^{(3)}(V) \sim \frac{\Delta}{g^2} \frac{1}{V^2}, \quad g^{-2} < |V|/\Delta < g^{-1}. \quad (10)$$

The averaged modulus of the matrix element in this case is $|V_{eff}^{(3)}| \sim \Delta \ln g/g^2$.

Higher-order effective matrix elements are obtained by simply adding more intermediate states to Eq. (9). Extensive discussions of the problems arising while calculating the averaged value of this matrix element may be found in Ref. [14]. For example, the averaged modulus of the four-particle effective matrix element for a given Feynman diagram is given by

$$|V_{eff}^{(4)}| = \left| \sum_{2,3} \frac{V_{12}V_{23}V_{34}}{\varepsilon_2\varepsilon_3} \right| = \frac{(\sqrt{2}\Delta)^3}{(\sqrt{\pi}g)^3} \int \frac{1}{|\varepsilon_2\varepsilon_3|} \frac{d\varepsilon_2}{2\Delta} \frac{d\varepsilon_3}{2\Delta}. \quad (11)$$

Here, compared to Eq. (9), we have made the change of variables $\varepsilon_1 - \varepsilon_2 \rightarrow \varepsilon_2$ and $\varepsilon_1 - \varepsilon_3 \rightarrow \varepsilon_3$. The preintegral factor $\sim (\Delta/g)^3$ in Eq. (11) arose after averaging the Gaussian distributed [Eq. (1)] direct matrix elements $|V_{ij}|$. The upper bound for both remaining integrals in Eq. (11) is given by the single-particle level spacing $|\varepsilon_{2,3}| < \Delta$. Due to the logarithmic character of the integrals, the order of magnitude estimate of the bounds is enough. More interesting is the origin of the bounds at small $\varepsilon_{2,3}$. Analogously to what we have discussed for the three-particle interaction, the formula (11) describes the mixing of four states $|1\rangle$, $|2\rangle$, $|3\rangle$, and $|4\rangle$ in the third order of perturbation theory. The interaction of the four states may be replaced by the effective interaction of only two states $|1\rangle$ and $|4\rangle$ if the admixture of intermediate states $|2\rangle$ and $|3\rangle$ is small. This requirement, for example, for state $|2\rangle$ means that $|\varepsilon_2| \gg |V_{12}| \sim \Delta/g$ (weak mixing of $|2\rangle$ and $|1\rangle$) and $|\varepsilon_2| \gg |V_{23}V_{34}/\varepsilon_3| \sim (\Delta/g)^2/|\varepsilon_3|$ (weak mixing of $|2\rangle$ and $|4\rangle$). Another two inequalities for the vector $|3\rangle$ are $|\varepsilon_3| \gg \Delta/g$ and $|\varepsilon_3| \gg (\Delta/g)^2/|\varepsilon_2|$. Combining all these inequalities, one finds for the range of integration in Eq. (11)

$$\Delta/g \ll |\varepsilon_{2,3}| \ll \Delta. \quad (12)$$

These bounds allow one to find the averaged matrix element with $\sim 1/\ln g$ accuracy: $|V_{eff}^{(4)}| \sim \Delta(\ln g)^2/g^3$. In a similar way one may consider the five-particle, six-particle, etc., effective interaction. Unfortunately, the system of inequalities describ-

ing the range of integration for the intermediate energies turns out to be sufficiently more complicated in these cases.

Formulas such as Eq. (11) may be used to find again the distribution of the effective matrix elements. In particular for the four-particle interaction

$$\overline{|V_{eff}^{(4)}|} = \int P^{(4)}(V_{eff}^{(4)}) dV_{eff}^{(4)},$$

$$P^{(4)}(V_{eff}^{(4)}) = \frac{(\sqrt{2}\Delta)^3}{(\sqrt{\pi}g)^3} \int \delta\left(V_{eff}^{(4)} - \frac{(\sqrt{2}\Delta)^3}{(\sqrt{\pi}g)^3} \frac{1}{\varepsilon_2\varepsilon_3}\right) \frac{d\varepsilon_2 d\varepsilon_3}{4|\varepsilon_2\varepsilon_3|\Delta^2}. \quad (13)$$

Here the range of variation of ε_2 and ε_3 is the same as in Eq. (11). Found in this way, the probability distribution in the general case has the form

$$P^{(n)}(V) \sim \frac{\Delta}{g^{n-1}} \frac{1}{V^2} \chi^{(n)}, \quad g^{-n+1} < |V|/\Delta < g^{-1}, \quad (14)$$

where $\chi^{(n)}(V)$ is a piecewise polynomial function of the order $n-3$ of two logarithms $\ln(|V|/\Delta)$ and $\ln g$. Again, in the simplest nontrivial example of $n=4$ one finds

$$\chi^{(4)} = \begin{cases} \ln(|V|g^3/\Delta), & g^{-3} < |V|/\Delta < g^{-2} \\ -\ln(|V|g/\Delta), & g^{-2} < |V|/\Delta < g^{-1}. \end{cases} \quad (15)$$

Also notice the huge range of variation of $V_{eff}^{(n)}$ [Eq. (14)] for large n . Averaging the matrix element over the distribution (14) leads to

$$\overline{|V_{eff}^{(n)}|} \sim \Delta (\ln g)^{n-1} / g^n. \quad (16)$$

Due to a complicated domain of integration over the intermediate energies it is difficult even to estimate the value of the overall numerical constant here. However, the important result of Ref. [14] is that at large n this unknown overall constant is neither large like $n!$ nor small like $1/n!$. The appearance of logarithms in the coefficients of the wave function was also observed in [19].

As in Eq. (7), the corrections generated by the many-particle effective interaction are naturally exponentiated at least for $n \ll T/\Delta$. Thus combining Δ_n [Eq. (8)] with $V_{eff}^{(n)}$ [Eq. (16)], we obtain instead of (7)

$$I = \exp\left\{-\frac{4\sqrt{3}}{\sqrt{\pi}g} \left(\frac{\mathcal{E}}{\Delta}\right)^{3/2} F\left(\frac{\ln g}{g} \frac{\mathcal{E}}{\Delta}\right)\right\},$$

$$F(x) = 1 + \sum F_n x^n. \quad (17)$$

In the case of the short-range screened two-particle interaction $V(\vec{r}_1, \vec{r}_2) \sim \delta(\vec{r}_1 - \vec{r}_2)$ the first coefficient here is $F_1 = 24\sqrt{2}/\pi^5$. This result for I may be compared with the perturbative result for the IPR for disintegration of the single quasiparticle in the isolated quantum dot found in Refs. [12–14]:

$$I_q = 1 - \frac{1}{\ln g} \phi(y), \quad \phi = \sum_{n=1}^{\infty} \phi_n y^n, \quad (18)$$

where $y = (\mathcal{E}/\Delta)^2 \ln g/g$ and \mathcal{E} is the energy of the quasiparticle. In analogy with the usual IPR, the I_q is a sum of fourth powers of the amplitudes to find a given k th quasi-particle in the i th exact state $I_q = \sum_i |\psi_i(k)|^4$. Section IV will be devoted to the more detailed investigation of the possible properties of the scaling function $F(x)$. For a single quasiparticle the coefficients ϕ_n decrease like $n!^{-1}$ for large n , which makes very improbable the disintegration of a quasiparticle through the delocalization transition in the Fock space.

The simple counting of the powers of \mathcal{E}/Δ and g in Eq. (17) leads to the following scenario of the development of chaos.

(a) For $\Delta g^{2/3} < \mathcal{E} < \Delta g/\ln g$ Eq. (7) is valid. The number of components in a typical wave function is exponentially large, but described by simple multiplication of independent direct transitions.

(b) At $\mathcal{E} \sim \Delta g/\ln g$ all terms in the series (17) enter the picture. The wave function is formed by a fractal combination of states distant in the Fock space [20]. If the resumed scaling function F is a regular function of the argument x (as it is for $\phi(y)$ [Eq. (18)]), the number of components of the wave function will be small compared to the total density of states and the level statistics will be close to Poissonian.

(c) Starting from $\mathcal{E} \sim \Delta g$, all quasiparticles constituting the wave function have enough energy to decay via the usual golden rule. Only here is the Wigner-Dyson statistics evident. The more formal criteria for onset of chaos will be the requirement that the product $I\mathcal{E}\nu_{total}$ become of the order of ~ 1 , where ν_{total} is the total density of states described above Eq. (2). This condition is equivalent to the equation for unknown function $F(x)$,

$$xF(x) = \frac{\pi\sqrt{\pi}}{6\sqrt{2}} \ln g. \quad (19)$$

The solution of this equation gives the energy of the transition to a rigid spectrum somewhere within $g/\ln g < \mathcal{E}/\Delta < g$. Due to the exponential character of I and ν_{total} most likely this will be the narrow phase transition.

IV. THE $N!$ SCENARIO

Thus the power counting for the perturbative IPR (17) may provide us with the formally self-consistent scenario of chaos developing in finite Fermi systems. Now we are going to show how taking into account of the high-order behavior of the coefficients F_n may lead to the important revision of this straightforward scheme. Unfortunately, we are not able to perform the complete estimation of the asymptotics of F_n . Nevertheless, the catastrophic change of the mechanism of the onset of chaos, which we will consider, may partly compensate for the lack of rigor. Therefore, even though based on certain assumptions, the result of this section should be considered as one of the main results of the paper.

The calculation of any term of the series in Eq. (17) consists of two main steps. First is the calculation of the density of final states, which we were able to perform explicitly [Eq. (8)]. The second step is the estimation of the effective matrix element. The matrix element for a given Feynman diagram is described by Eq. (16). As we have said, this matrix element could not contain any $n!$ or $n!^{-1}$. However, for the many-

body problem and high order of perturbation theory the same initial and final configurations may be connected by many different Feynman diagrams. We have shown in Fig. 2 the example of the corresponding tree-type n -particle diagram. The total number of diagrams N_d , like in Fig. 2, is

$$N_d = n^{n-2}(n-1)n!. \quad (20)$$

Here $n!$ is the number of permutations of $1'-n'$ final particles, $(n-1)!$ is the number of replacements of (screened) Coulomb interaction lines, and n^{n-2} is the number of $(n-1)$ -segment trees connecting n points $1-n$ [21]. Equation (20) gives us the number of diagrams of the Schrödinger perturbation theory. Among the N_d trees there are many diagrams having the same set (up to permutations) of matrix elements of the two-particle interaction V_{ij} and different energy denominators. As it was pointed out in Ref. [14], these diagrams could not be considered as statistically independent, which results in lowering of the mixing by the high-order effective interaction. The averaged modulus of the effective matrix element found for the single Feynman diagram (16) should be modified in the case of many interfering diagrams. However, due to a huge range of variation of the V_{eff} in the power law distribution (14), the average value is saturated by a rare very large fluctuation of the matrix element. Therefore, for n not too large the generalization of Eq. (16) for the many-diagram case is achieved by the simple multiplication by the number of diagrams (we will return later to the discussion of very large n). Finally, combining Eqs. (8), (16), and (20), we find

$$F_n \leq n!. \quad (21)$$

We see that the series in Eq. (17) most likely is the asymptotic series. Due to the unsatisfactory estimate of the number of diagrams and even the value of the individual diagram, we were able to draw only the upper bound for F_n . However, it seems very unlikely that the cancellation between the diagrams of the Schrödinger perturbation theory will remove the factorial divergence of the coefficients of the series. In the following (unless explicitly indicated otherwise) we suppose that $F_n \sim n!$. The asymptotic series, common in field theory and high energy physics, usually do not cause serious troubles (for a review see Ref. [22]). In all known cases one simply breaks the summation on the smallest term of the series and uses this smallest term also as the order of magnitude estimate of the rest of the nonperturbative part of the sum. The more refined strategy will be to perform the Borel summation, but this procedure (up to the same nonperturbative corrections) is equivalent to the breaking of the series at the smallest term. In our example this means that one should break the summation in Eq. (17) at $n_0 \sim g \Delta / \ln g \mathcal{E}$ and the nonperturbative ambiguity in F should be

$$\delta F_{np} \sim e^{-n_0} \sim \exp \left\{ -\sigma \frac{g}{\ln g} \frac{\Delta}{\mathcal{E}} \right\}, \quad (22)$$

with some $\sigma \sim 1$. However, in the known field-theoretic examples there exist clear physical mechanisms (instanton and renormalon) that allow us to understand the origin of nonperturbative corrections and the necessity of breaking the

series at the smallest term. In our many-body quantum problem we could find *no physical motivation for the appearance of nonperturbative corrections of the kind (22) and we see no reasons for breaking the summation in Eq. (17) at the smallest term*. Of course, Eq. (17) is not exact, but corrections to $F(x)$ are small, e.g., $(\ln g)^{-1}$ or Δ/\mathcal{E} . Taking into account such corrections will help us sum up the original divergent series. Nevertheless, in order to make sense of our perturbative analysis of the onset of chaos in finite Fermi systems we should find the physically motivated cutoff for the $n!$ divergent sum. The natural cutoff for F_n , which we see, is given by the total number of particles that may enter the diagram of the effective interaction $n_{max} \sim T/\Delta \sim \sqrt{\mathcal{E}/\Delta}$. If $n_{max} > x^{-1}$ the summation now goes above the smallest term of the series. The consequences of the decision to sum up the series above the smallest term are crucial. In the standard scheme the function $F(x)$ is described by perturbation theory at small x and becomes completely nonperturbative (although it still may be smooth and finite) at $x \sim 1$. Within the new scenario $F(x)$ blows up at

$$F_{n_{max}} x^{n_{max}} \sim (n_{max} \ln g \mathcal{E} / g \Delta)^{n_{max}} \sim 1, \quad (23)$$

which gives the chaotization threshold $\mathcal{E}_c \sim \Delta (g/\ln g)^{2/3}$. This estimate was done for the most strongly divergent series allowed by Eq. (21). For example, if $F_n \sim (n/2)!$ the same calculation will lead to $\mathcal{E}_c \sim \Delta (g/\ln g)^{4/5}$. Therefore, the more accurate conclusion from Eq. (21) is that due to the effective interaction including all $\sim T/\Delta$ excited particles, the series for the IPR (7) blows up at some $(g/\ln g)^{2/3} < \mathcal{E}_c < g/\ln g$ [23].

Two important peculiarities of the emergence of quantum chaos follow from this ‘‘factorial’’ scenario.

(i) The direct interaction connects only the states close in the Fock space [20]. Therefore, Eq. (7) describes mixing of only a small part of close levels. On the other hand, the highest-order effective interaction entering Eq. (23) mixes the huge number (the majority of all many-particle excitations) of very distant simple states. Thus divergence of $F(x)$ due to $n!$ leads to the transition from the Poisson to the rigid (Wigner-Dyson) spectrum at $\mathcal{E} = \mathcal{E}_c$.

(ii) Due to the large power of x in Eq. (23), the growth of $F(x)$ with the increase of energy takes place at a very narrow interval $\Delta \mathcal{E} / \mathcal{E}_c \sim 1/n_{max}$. This means that the change of statistics has a form of phase transition with relative width $\sim 1/n_{max}$.

Our description of the development of chaos is sufficiently based on the estimate of n_{max} [Eq. (23)]. If one is able to find another reason for breaking the series at a term parametrically smaller than $n_{max} \sim T/\Delta$ the result for \mathcal{E}_c also will be different. For example, the new cutoff may arise due to a huge number of interfering diagrams (20). The joint probability distribution for the sum of many diagrams with power-law individual distributions described by Eq. (14) has a Lorentzian form [24] with the width γ having the form

$$P(V) \sim \frac{\gamma}{V^2 + \gamma^2} \frac{\chi(V)}{\chi(\gamma)}, \quad \gamma \sim \chi(\gamma) \frac{\Delta N_d}{g^{n-1}} \sim \Delta \frac{n^{3n}}{g^n}. \quad (24)$$

Here we have used for the estimate of the number of independent diagrams the upper bound (20). This distribution is

valid for $|V| < \Delta/g$. The function χ was defined in Eq. (14). The factor $\chi(V)/\chi(\gamma)$ allows us to preserve the asymptotics (14) at $|V| \gg \gamma$. Due to the logarithmic character of χ , this factor correctly accounts for the deviation from the pure power law in the distribution of single matrix elements. We see that after taking into account the interference of different diagrams, the power-law distribution of the total matrix element becomes strongly violated at $|V| \sim \gamma$, not at $|V| \sim \Delta g^{-n+1}$ as in Eq. (14). The value of F_n found with the distribution $P(V)$ [Eq. (24)] becomes parametrically different from the estimate (21) only at $n'_{max} \sim g^{1/3}$ [even at $n'_{max} \sim (g/\ln g)^{1/3}$ if one considers seriously the high powers of logarithms in Eq. (24)]. However, this new variant of the cutoff leads to the same threshold for the onset of chaos as we have found before in Eq. (23). This coincidence of the results of two different approaches to the estimation of n_{max} may be considered as indirect support for the transition to Wigner-Dyson statistics at $\mathcal{E}_c \sim \Delta(g/\ln g)^{2/3}$.

At least some of the thresholds shown in Fig. 1 may lie above \mathcal{E}_c . The physical meaning of these perturbative thresholds becomes less clear. Nevertheless, even above \mathcal{E}_c one may try to look for effects generated by the direct or low-order effective interaction. The highest-order effective interaction becomes important due to the huge combinatorics (20), but the corresponding matrix element is in general very small (up to $V \sim \Delta/g^{n_{max}}$). Thus this high-order interaction may be invisible (or at least suppressed) at small times in time-dependent problems. For example, one may consider the time evolution of the wave packet $\Psi(t)$, starting at $t = 0$ from a single Slater determinant. The pure direct interaction in this case gives

$$|\langle \Psi(0) | \Psi(t) \rangle|^2 = e^{-\Gamma t}, \quad \Gamma = 2\sqrt{6}\Delta g^{-2}(\mathcal{E}/\Delta)^{3/2}. \quad (25)$$

The formal power counting [like we have done below Eq. (17)] gives for the range of validity of this result $\Delta g^{2/3} \ll \mathcal{E} \ll \Delta g/\ln g$. However, due to the logarithmic behavior of all integrals [see, e.g., Eq. (11)] all values of the high-order effective matrix elements are equally important within $g^{-n+1} < |V|/\Delta < g^{-1}$ [Eq. (14)]. Therefore, the range of validity of Eq. (25) may change greatly after taking into account the contribution from large high-order effective matrix elements.

V. DISCUSSION

The goal of this paper was to consider how the chaotic mixing of noninteracting eigenstates develops with increasing the excitation energy in finite weakly interacting Fermi systems. Measured in units of the single-particle level spacing Δ the energy corresponding to the onset of rigid spectrum may depend on only one parameter g [Eq. (1)]. Nevertheless, even with only one parameter we were able to introduce a number of different energy scales, shown in Fig. 1, which correspond to (or may correspond to) the different stages of development of chaos.

The low lying thresholds in the figure $\varepsilon/\Delta \sim (g/\ln g)^{1/2}$ and $\varepsilon/\Delta \sim g^{1/2}$ are associated with the decay of a single quasiparticle. These thresholds were considered in Refs. [10–14] and their description was not the aim of this paper. However, the methods introduced in Refs. [12,14] for the investigation

of below golden rule decay provides us with a useful tool for the investigation of the onset of chaos in complex many-particle excitations also.

Technically, our consideration is based on the two simple equations (5) and (7) for the IPR. The two noninteracting states are strongly mixed by the interaction if the corresponding energy difference turns out to be of the same order of magnitude as the matrix element. As a result, all the effects that we consider are determined by the product of the averaged modulus of the matrix element and the density of accessible states.

The emergence of chaos in the majority of complicated states with many excited particles and holes was the main subject of this paper. This increase of chaos with the growth of excitation energy proceeds in a very complicated way, both technically and especially logically. In the simplest variant, mixing of the simple (single Slater determinant) states is caused by the direct interaction. The mixing by direct interaction starts at $\mathcal{E} > \Delta g^{2/3}$ [25]. Due to the large number of excited particles, the interaction may proceed through a large number of independent channels. This results in the exponentiation of the IPR, as we have shown at the end of Sec. II. Thus, even the direct interaction may mix together an exponentially large number of Slater determinant configurations. However, this number is still small compared to the total number of levels of the complicated system and the direct interaction could not cause the transition from Poisson to Wigner-Dyson statistics of energy levels.

An alternative to the direct interaction is the transition via effective three-particle, four-particle, etc., interactions considered in Sec. III. The effect of this high-order interaction is much weaker than that of the direct interaction at low energies, but they became comparable at $\mathcal{E} \sim \Delta g/\ln g$. Above the energy $\mathcal{E} \sim \Delta g/\ln g$ our perturbative approach is no longer valid and we were forced to introduce the unknown scaling function $F(\ln g \mathcal{E}/g \Delta)$ into the exponent describing the IPR in Eq. (17). However, if one expects that $F(x \sim 1) \sim 1$, the logarithm of the number of components in the typical wave function at $\mathcal{E} \sim \Delta g/\ln g$ will be $\ln g \gg 1$ times smaller than the logarithm of the total number of states. This means that even though the mechanism of mixing changes and the number of components in the wave function increases much faster at $\mathcal{E} \sim \Delta g/\ln g$, this threshold does not correspond to the Poisson-Wigner-Dyson transition.

The Wigner-Dyson statistics become evident only at $\mathcal{E} \sim \Delta g$. This energy is analogous to the golden rule threshold $\varepsilon \sim \Delta g^{1/2}$ for the decay of a single quasiparticle. Roughly speaking, above the $\mathcal{E} \sim \Delta g$ any particle from the strip $\sim T$ around ε_F may decay via the golden rule.

Formally, in order to understand how the change of statistics proceeds between $\mathcal{E} \sim \Delta g/\ln g$ and $\mathcal{E} \sim \Delta g$ one should analyze the high-order behavior of the coefficients F_n in the expansion of the function $F(x)$ [Eq. (17)]. Surprisingly, this analysis in Sec. IV instead of such an understanding led us to the crucial revision of the straightforward scheme considered above.

As we have shown in Sec. IV, the series in Eq. (17) most likely is the asymptotic series. Although $F_n \sim n!$ [Eq. (21)] is only the upper bound for F_n , it seems very unlikely that the factorial divergence of the coefficients will be eliminated. Moreover, even if $F_n \sim (\nu n)!$ with any $0 < \nu < 1$, the results

of Sec. IV will be only slightly modified. The factorial divergence of the series would not be dangerous if one sums it up, e.g., via some variant of the Borel method. However, within the Borel prescription one is immediately faced with the problem of strange nonperturbative corrections like in Eq. (22) (moreover, that the F_n are positive by construction and the series is non-Borel summable). Being unable to find the physical motivation for the Borel summation, we were looking for another way to make sense of the divergent series. The coefficient F_n is given by the sum of $(n+1)$ st-order tree-type Feynman diagrams. Therefore, the natural cutoff for the series is given by the order of the largest diagram that may be constructed with available $\sim T/\Delta$ particles, namely, $n_{max} \sim T/\Delta$ (one more way to determine n_{max} considered in Sec. IV leads to the same physical result). Within this scenario the n_{max} and the scaling parameter $x = \ln g\mathcal{E}/g\Delta$ in Eq. (17) are two independent variables. At $x > 1/n_{max}$ the summation in Eq. (17) goes above the smallest term. However, up to the energy $\mathcal{E}_c \sim \Delta(g/\ln g)^{2/3}$ all n_{max} terms of the series are small. At $\mathcal{E} = \mathcal{E}_c$ even the broken series blows up and above \mathcal{E}_c our perturbative approach is no longer valid. Because the growth of $F(x)$ at $\mathcal{E} \approx \mathcal{E}_c$ proceeds mostly due to the last terms of the series or the most complicated diagrams of the highest allowed order of perturbation theory, this threshold corresponds to the narrow phase transition from the Poisson to the Wigner-Dyson spectrum. We attempted at the end of Sec. IV to find remnants of nonchaotic behavior above \mathcal{E}_c by considering the short time processes. However, this issue requires a separate and more careful investigation.

To summarize, we have considered in this paper the two scenarios how quantum chaos may develop in the finite Fermi systems depending on the way one uses the summation of factorially divergent contributions from the high-order effective interaction.

(i) If the series is summed up within the Borel prescription (i.e., broken effectively at the smallest term) we are able to find a few distinct stages of chaotic behavior. Below the energy $\sim \Delta g^{2/3}$ the majority of eigenvectors are almost un-

perturbed. Between $\sim \Delta g^{2/3}$ and $\sim \Delta g/\ln g$ a direct interaction mixes together the exponentially large number of simple states (7). However, the IPR is under theoretical control in this region and the statistics is clearly Poissonian. Above $\Delta g/\ln g$ the statistics of the energy levels is still Poissonian, but the IPR is described by some (unknown) scaling function $F(x)$ [Eq. (17)]. The transition to the Wigner-Dyson spectrum takes place somewhere between $\mathcal{E} \sim \Delta g/\ln g$ and $\mathcal{E} \sim \Delta g$ [see Eq. (19)]. The transition may be relatively narrow $\Delta\mathcal{E}/\mathcal{E} \sim (\ln g)^{-1}$.

(ii) In the second variant the cutoff of the series in Eq. (17) is determined by the number of particles in the largest allowed Feynman diagram and is independent of the scaling variable x . In this case the transition to the Wigner-Dyson spectrum takes place at $\mathcal{E}_c \sim \Delta(g/\ln g)^{2/3}$ and is narrow like $\Delta\mathcal{E}/\mathcal{E} \sim \Delta/T \sim (\ln g/g)^{1/3}$.

To our current understanding, the second scenario is more physically motivated. However, our argumentation in this part is not completely rigorous and one still may find reasons for summation of the tree diagrams in the manner of Borel. The important disadvantage (or perhaps advantage) of the second scheme is that if it is correct, it will be probably an example of the phase transition caused by the factorial divergence of the series. Finally, although both of our scenarios make physical predictions, we were able to make only the order of magnitude estimates of the considered thresholds. Therefore, any experimental confirmation (within the true experiment or by numerical simulations) of the mechanisms of the development of chaos considered in this paper is very desirable.

ACKNOWLEDGMENTS

The author is thankful for discussions with V.F. Dmitriev, V.V. Flambaum, A.A. Gribakina, G.F. Gribakin, I.V. Ponomarev, D.V. Savin, V.V. Sokolov, O.P. Sushkov, V.B. Telitsin, and A.S. Yelkhovskiy. The work has been supported in part by the Gordon Godfrey Foundation and by RFBR under Grant No. 98-02-17905.

-
- [1] E. P. Wigner, Ann. Math. **62**, 548 (1955); **65**, 203 (1957).
 [2] J. B. French and S. S. M. Wong, Phys. Lett. **33B**, 447 (1970); **35B**, 5 (1971).
 [3] O. Bohigas and J. Flores, Phys. Lett. **34B**, 261 (1971); **35B**, 383 (1971).
 [4] M. Horoi, V. Zelevinsky, and B. A. Brown, Phys. Rev. Lett. **74**, 5194 (1995); V. Zelevinsky, B. A. Brown, N. Frazier, and M. Horoi, Phys. Rep. **276**, 85 (1996).
 [5] V. V. Flambaum, G. F. Gribakin, and F. M. Izrailev, Phys. Rev. E **53**, 5729 (1996).
 [6] D. Weinmann, J.-L. Pichard, and Y. Imry, J. Phys. (France) I **7**, 1559 (1997).
 [7] Ph. Jacquoud and D. L. Shepelyansky, cond-mat/9706040; B. Georgeot and D. L. Shepelyansky, cond-mat/9707231.
 [8] T. Guhr, A. Müller-Groeling, and H. A. Weidenmüller, Phys. Rep. **299**, 189 (1998).
 [9] U. Sivan, F. P. Milliken, K. Milkove, S. Rihston, Y. Lee, J. M. Hong, V. Boegli, D. Kern, and M. deFranza, Europhys. Lett. **25**, 605 (1994).
 [10] U. Sivan, Y. Imry, and A. G. Aronov, Europhys. Lett. **28**, 115 (1994).
 [11] Ya. M. Blanter, Phys. Rev. B **54**, 12 807 (1996).
 [12] B. L. Altshuler, Y. Gefen, A. Kamenev, and L. S. Levitov, Phys. Rev. Lett. **78**, 2803 (1997).
 [13] A. D. Mirlin and Y. V. Fyodorov, Phys. Rev. B **56**, 13 393 (1997).
 [14] P. G. Silvestrov, Phys. Rev. Lett. **79**, 3994 (1997).
 [15] We suppose that the Fermi energy is large compared to the excitation energy $\varepsilon_F \gg \mathcal{E}$. The number of particles goes to infinity, but experimental accuracy still allows us to resolve individual energy levels (the mesoscopic limit).
 [16] A. Bohr and B. R. Mottelson, *Nuclear Structure* (Benjamin, New York, 1969), Vol. 1, p. 284.
 [17] The temperature and total energy may be easily related via $\mathcal{E} = \int (\varepsilon - \varepsilon_F) \bar{n}(\varepsilon) d\varepsilon / \Delta$.

- [18] I. V. Ponomarev and P. G. Silvestrov, Phys. Rev. B **56**, 3742 (1997).
- [19] V. V. Flambaum and F. M. Izrailev, Phys. Rev. E **56**, 5144 (1997).
- [20] We use the concept of the distance in the Fock space introduced in Ref. [12]. The distance between two simple states equals one if they are related by the direct interaction in the first order of perturbation theory.
- [21] This combinatorial calculation was done by Cayley more than a century ago. The author is thankful to A. Gribakina and G. Gribakin for a discussion of this result.
- [22] *Large Order Behavior of Perturbation Theory*, edited by L. C. Le Guillou and J. Zinn-Justin (North-Holland, Amsterdam, 1990).
- [23] Only if the factorial divergence of F_n is washed out completely due to the large number of coinciding diagrams in Eq. (20) (which seems very unlikely) will \mathcal{E}_c be raised again to that predicted by Eq. (19).
- [24] See, for example, P. A. Mello, in *Mesoscopic Quantum Physics*, 1994 Les Houches Lectures, Session LXI (Elsevier, Amsterdam, 1995), Appendix B.
- [25] In particular this means that the decay of single quasiparticles starts at parametrically lower energies than the mixing of complicated many-particle excitations ($\Delta g^{1/2} \ll \Delta g^{2/3}$). Thus, below the energy $\varepsilon \sim \Delta g^{2/3}$ one may consider the decay of the quasiparticle (via the golden rule or otherwise) into almost nonperturbed few particle states as it was done in Refs. [10–14].